Interfacial Behavior of Compressible Polymer Blends. Monte Carlo Simulation and the Lattice Fluid Theory

G. J. A. Ypma,[†] P. Cifra,*[,‡] E. Nies,[†] and A. R. D. van Bergen[§]

Eindhoven Polymer Laboratories, Faculty of Chemical Engineering, Eindhoven University of Technology, P.O. Box 513, 5600 MB Eindhoven, The Netherlands, Polymer Institute, Slovak Academy of Sciences, 842 36 Bratislava, Slovakia, and Shell Research Amsterdam, Equipment Engineering Department, P.O. Box 38000, 1030 BN Amsterdam, The Netherlands

Received July 5, 1995; Revised Manuscript Received November 6, 1995[⊗]

ABSTRACT: Monte Carlo (MC) lattice simulation studies have been performed for compressible polymer−polymer interfaces showing a density dip at the interface of an immiscible polymer pair. The dependence of the interfacial properties on the cross interaction energy and pressure is investigated. The simulations are compared with theoretical calculations. Therefore a theory is developed using the lattice fluid (LF) theory applied to polymer interfaces according to Helfand's ideas, using anisotropy factors (probabilities) for the polymer bond directions to account for the inhomogeneity at the interface. The free energy is expressed in terms of these anisotropy factors, polymer densities, and segment−segment contact energies. It is minimized under a number of constraints using the technique of Lagrange multipliers. Between simulations and theory a gratifying qualitative agreement is found. Systems asymmetric in density can be treated, which is important for application to real systems. Application of Helfand's lattice approach is not restricted to broad interfaces and therefore presents a good alternative to gradient term interface theories.

I. Introduction

Surface and interface properties are important for many technological applications of polymers. They play a significant role in thermoplastic processing, coating, film production, and using polymers as adhesives. Apart from theoretical interest in the compressible interfaces, generally, the existence of the density dip at the interface can have more applied consequences, for instance in the mechanical properties of heterogeneous polymer materials where transfer of stress across the interface plays a key role in the performance of these materials.

In the past, several theories have been developed to describe the behavior of polymers in inhomogeneous systems and at surfaces in particular. Most of the theories originate from the work of Flory and Huggins,[1,2] and for a long time consistently invoked the simplifying incompressibility assumption.

Helfand used Flory's original lattice theory and introduced anisotropy factors to account for the inhomogeneity at the interface.[3−5] Poser and Sanchez[6] used Flory's lattice theory in conjunction with the Cahn−Hilliard theory.[7,8] They expressed the Helmholtz free energy in terms of an expansion in density (assuming small gradients) and neglected conformational entropy effects which are essential for long polymer molecules. They described the polymer chain using Gaussian random-walk (GRW) statistics.

Recent theories do include compressibility. One, developed by Hong and Noolandi,[9] is based on Helfand's functional integral approach,[10] uses a partition function written as a functional integral over the density, and accounts for conformational entropy effects. It yields the Sanchez−Lacombe (or lattice fluid) equation of state.[11] The other, by Lifschitz and Freed,[12] uses the lattice fluid theory with the de Gennes modified square gradient coefficient.[13] Its computations, so far, are limited to symmetric blends. Other investigations of several research groups have incorporated the Sanchez−Lacombe equation of state theory in self-consistent theoretical calculations. In these studies the thermodynamic and structural properties of the solid wall/polymer interface as well as the free surface of pure polymers and polymer blends were considered.[14,15]

In more recent theoretical work density functional theory has been applied to study inhomogeneous systems. The density functional technique which has proven to be valuable for atomic systems[16] has been extended to polyatomic systems as well.[17] Recent applications related to the problems discussed here are concerned with polymer fluids at a wall.[18]

In this work we extend the lattice fluid theory to inhomogeneous systems and to polymer−polymer interfaces in particular, using the anisotropy factors introduced by Helfand. This approach does not have the small gradient restriction and can therefore be used to calculate sharp interfaces. For slowly varying gradients the results reduce to those of the GRW models. Another advantage is that it is computationally simple and systems asymmetric in density can be treated.

Monte Carlo simulation results for compressible polymer−polymer interfaces using a lattice model are presented and compared with LF theoretical calculations, both the LF model and the MC simulations use the same molecular model, i.e. lattice chains with nearest neighbor interactions. First the basic definitions and principles of the LF theory are given. The next section shows how the theory is applied to treat polymer interfaces. After a brief review of the MC simulation method, the results for immiscible polymer−polymer interfaces are presented and compared to the theory in the last section.

II. Theory

II.a. Lattice Fluid Theory. In the lattice fluid theory a lattice of coordination number z with a total

[†] Eindhoven University of Technology.
[‡] Slovak Academy of Sciences.
[§] Shell Research Amsterdam.
[⊗] Abstract published in *Advance ACS Abstracts,* January 1, 1996.

0024-9297/96/2229-1252$12.00/0

number of N_t sites is used to enumerate the number of configurations Ω available to a system of k polymer components, each of N_i molecules and N_v voids or empty sites. A molecule occupies s_i sites on the lattice. The total volume of the lattice is $V = N_t v^*$ where v^* is the volume of one lattice site. The site fraction in the absence of voids ϕ_i is defined as

$$\phi_i = \frac{s_i N_i}{sN} \qquad s = \frac{\sum s_i N_i}{\sum N_i} = \frac{\sum s_i N_i}{N} \tag{1}$$

where s is the average number of segments per molecule, N is the total number of polymer molecules, and hence sN is the total number of polymer segments. The reduced density $\tilde{\rho}$ or the fraction of sites occupied by all polymer molecules is equal to the reciprocal of the reduced volume

$$\tilde{\rho} = \frac{sN}{N_v + sN} \equiv 1/\tilde{v} \tag{2}$$

the site fraction occupied by segments of type i is

$$\varphi_i = \frac{s_i N_i}{N_v + sN} = \phi_i \tilde{\rho} = \phi_i/\tilde{v} \tag{3}$$

and the void fraction φ_v is given by

$$\varphi_v = \frac{N_v}{N_v + sN} = 1 - \tilde{\rho} = 1 - \sum_{i=1}^{k} \varphi_i \tag{4}$$

The thermodynamic behavior of the molecules is embodied in the Helmholtz free energy, combining entropy S and energy E.

$$A = E - TS \tag{5}$$

The entropic contribution is the combinatorial or configurational entropy calculated from the total number of arrangements Ω of the molecules on the lattice.

$$S = k_B \ln \Omega \tag{6}$$

where k_B represents the Boltzmann constant. Although in reality this arrangement is affected by the energetic interactions between molecules, it is calculated without regard to these interactions, leading to a random mixing of the segments. Using the Flory approximation[2] for the number of arrangements, Stirling's approximation ($N! = (N/e)^N$) and the definitions given above yield

$$-S/k_B = sN\left(\frac{(1-\tilde{\rho})}{\tilde{\rho}}\ln(1-\tilde{\rho}) + \frac{1}{s}\ln\tilde{\rho} + \sum_{i=1}^{k}\frac{\phi_i}{s_i}\ln\left(\frac{\phi_i}{\omega_i}\right)\right) \tag{7}$$

The density dependent terms of this equation can be interpreted as the increase in entropy associated with mixing molecules and voids. The ω_i term deals with the intramolecular conformations of the chains and is constant for homogeneous systems;[11] however, this term becomes very important when the theory is applied to inhomogeneous systems such as interfaces.

The second contribution to the Helmholtz free energy is the attractive energy term or simply the energetic term, calculated as the product of the number of contacts in the system and a characteristic interaction energy per segment−segment contact. Only nearest neighbor interactions are considered, hence the total contact energy E, counting paired segments with a constant interaction energy, is given by

$$E = -\sum_{i=1}^{k}\sum_{j=1}^{k} p_{ij}\epsilon_{ij} \tag{8}$$

where p_{ij} is the total number of $i-j$ contact pairs given by

$$p_{ii} = s_i N_i z \varphi_i/2 \tag{9}$$

$$p_{ij} = s_i N_i z \varphi_j \tag{10}$$

For a two-component (A and B) system the energetic term is now given by

$$\begin{aligned} E/k_B T &= -\Big[s_A N_A \varphi_A \frac{z}{2}\epsilon_{AA} + s_B N_B \varphi_B \frac{z}{2}\epsilon_{BB} + 2 s_A N_A \varphi_B \frac{z}{2}\epsilon_{AB}\Big]/k_B T \\ &= -sN\tilde{\rho}\frac{z}{2k_B T}[\phi_A{}^2\epsilon_{AA} + \phi_B{}^2\epsilon_{BB} + 2\phi_A\phi_B\epsilon_{AB}] \\ &= -sN\tilde{\rho}\frac{T^*}{T} \end{aligned} \tag{11}$$

where T^* is the so-called scaling temperature:

$$k_B T^* = \frac{z}{2}[\phi_A{}^2\epsilon_{AA} + \phi_B{}^2\epsilon_{BB} + 2\phi_A\phi_B\epsilon_{AB}] \tag{12}$$

From eqs 7 and 11, for a two-component polymer system the Helmholtz free energy is given by

$$\frac{A}{sNk_B T} = \frac{\phi_A}{s_A}\ln(\phi_A) + \frac{\phi_B}{s_B}\ln(\phi_B) + \frac{1}{s}\ln(\tilde{\rho}) + \frac{(1-\tilde{\rho})}{\tilde{\rho}}\ln(1-\tilde{\rho}) - \frac{\tilde{\rho}}{\tilde{T}} \tag{13}$$

Note that ω_i has been omitted; for homogeneous systems it is independent of composition and has no influence on phase equilibria or the equation of state.

From thermodynamics it is known that

$$-P = \left(\frac{\partial A}{\partial V}\right)_{N_1,N_2,T} = \frac{1}{v^*}\left(\frac{\partial A}{\partial N_v}\right)_{N_1,N_2,T} \tag{14}$$

This derivative yields the Sanchez−Lacombe equation of state which for infinitely long molecules ($s = \infty$) reads (after some rearrangements)

$$-\frac{Pv^*}{k_B T} = -\frac{\tilde{P}}{\tilde{T}} = \tilde{\rho} + \ln(1-\tilde{\rho}) + \frac{\tilde{\rho}^2}{\tilde{T}} \tag{15}$$

The theory given above provides the bulk properties of compressible isotropic systems and is not applicable to inhomogeneous systems involving, e.g., interfaces. The reduced parameters used in the theory are related to the experimental temperature T, pressure P, and density ρ according to

$$\tilde{T} \equiv \frac{T}{T^*} \qquad \tilde{P} \equiv \frac{P}{P^*} \qquad \tilde{\rho} \equiv \frac{\rho}{\rho^*} \tag{16}$$

The reduced parameters can be determined from experimental PVT data and are tabulated for a large number of polymers.

II.b. Application to Interfaces: The Helfand Approach. To describe immiscible polymers at interfaces, Helfand[3] starts from the original lattice theory as described by Flory[1] where a lattice is fully occupied and hence incompressibility is assumed. The lattice is regarded as consisting of layers l, each containing n_s

sites. Each site of the lattice has z nearest neighbors, a fraction m neighbors in an adjoining layer and a fraction $(1 - 2m)$ in the same layer. The polymer molecules will be taken as being of infinite molecular weight, hence consisting of identical segments (chain ends are ignored). If A−A and B−B segment contacts are chosen to be sufficiently more favorable then A−B contacts, there is an effective repulsion between A and B segments, and two phases will coexist across an interface. The mathematical manifestation is that the layers have a fractional occupancy $\varphi_{l\mathrm{K}}$ of species K in layer l, which is constant for many layers and decreases to become zero in the bulk of the other polymer. The φ's must be chosen so as to minimize the free energy of the system to meet equilibrium conditions at a given T and V. The free energy A^{inh} of the inhomogeneous system is defined as

$$A^{\mathrm{inh}} = E^{\mathrm{inh}} - TS^{\mathrm{inh}} \tag{17}$$

For infinitely long molecules ($s = \infty$) S^{inh} is the contribution of the conformational entropy, associated with the loss of conformational freedom resulting from molecules near the interface having to turn back from the opposite phase. E^{inh} is the contribution of the contact energy between segments.

Due to the inhomogeneity a dependency is expected on the species of the chain K = A or B, the layer l from which a bond emanates, and the direction of the bond. In the simple cubic lattice model this direction can be specified by an anisotropy factor $g^{\nu}{}_{l\mathrm{K}}/z$, where ν gives the direction with label +, 0, or −;

$\nu = +$ if the (layer of segment$_{n+1}$) − (layer of segment$_n$) $= +1$

$\nu = 0$ if the (layer of segment$_{n+1}$) − (layer of segment$_n$) $= 0$

$\nu = -$ if the (layer of segment$_{n+1}$) − (layer of segment$_n$) $= -1$

This anisotropy factor reduces to unity in the bulk; a value greater than 1 indicates a greater than random tendency for bonds of K with an end on layer l to point in the ν direction.

The following expression for the entropic contribution can be derived:[3−5]

$$S^{\mathrm{inh}} = -k_{\mathrm{B}}n_{\mathrm{s}}\sum_{K=A,B}\sum_{l}\varphi_{l\mathrm{K}}[mg^{+}{}_{l\mathrm{K}}\ln g^{+}{}_{l\mathrm{K}} + (1-2m)g^{0}{}_{l\mathrm{K}}\ln g^{0}{}_{l\mathrm{K}} + mg^{-}{}_{l\mathrm{K}}\ln g^{-}{}_{l\mathrm{K}}] - k_{\mathrm{B}}n_{\mathrm{s}}\sum_{l}\varphi_{l\mathrm{v}}\ln\varphi_{l\mathrm{v}} \tag{18}$$

The last term results from the increased number of configurations due to the presence of voids.

If random mixing is assumed, the energetic contribution to the free energy is derived by counting the segment−segment contacts on the lattice. For example an A type segment in layer l has $z(1 - 2m)$ contacts in the same layer and a probability that one of these contacts is an A or a B type is related to the segment fraction in that layer (see also eq 11). The segment has zm contacts in an adjoining layer. Summing all segments in a layer and over all layers gives

$$E_{l,l} = \sum_{l} n_{\mathrm{s}}z(1-2m)(\varphi_{l\mathrm{A}}{}^{2}\epsilon_{\mathrm{AA}} + \varphi_{l\mathrm{B}}{}^{2}\epsilon_{\mathrm{BB}} + 2\varphi_{l\mathrm{A}}\varphi_{l\mathrm{B}}\epsilon_{\mathrm{AB}}) \tag{19}$$

$$E_{l,l-1} = \sum_{l} n_{\mathrm{s}}zm(\varphi_{l\mathrm{A}}\varphi_{l-1,\mathrm{A}}\epsilon_{\mathrm{AA}} + \varphi_{l\mathrm{B}}\varphi_{l-1,\mathrm{B}}\epsilon_{\mathrm{BB}} + \varphi_{l\mathrm{A}}\varphi_{l-1,\mathrm{B}}\epsilon_{\mathrm{AB}} + \varphi_{l\mathrm{B}}\varphi_{l-1,\mathrm{A}}\epsilon_{\mathrm{AB}}) \tag{20}$$

$$E_{l,l+1} = \sum_{l} n_{\mathrm{s}}zm(\varphi_{l\mathrm{A}}\varphi_{l+1,\mathrm{A}}\epsilon_{\mathrm{AA}} + \varphi_{l\mathrm{B}}\varphi_{l+1,\mathrm{B}}\epsilon_{\mathrm{BB}} + \varphi_{l\mathrm{A}}\varphi_{l+1,\mathrm{B}}\epsilon_{\mathrm{AB}} + \varphi_{l\mathrm{B}}\varphi_{l+1,\mathrm{A}}\epsilon_{\mathrm{AB}}) \tag{21}$$

When the above equations are summed, every contact is counted twice; hence for the total energy of mixing we get

$$E^{\mathrm{inh}} = \frac{1}{2}(E_{l,l} + E_{l,l+1} + E_{l,l-1}) \tag{22}$$

This expression holds for the incompressible case as well because the interaction between voids and between polymer segments and voids is assumed to be zero.

To determine the polymer density profiles and the anisotropy factors, the free energy has to be minimized subject to a number of constraints using the technique of Lagrange multipliers. The constraints for this problem are given below; they are slightly different from those in the incompressible problem (compare to eqs 4.3−4.5 in ref 3):

	constraint	Lagrange multiplier
1. full occupancy	$\varphi_{l\mathrm{A}} + \varphi_{l\mathrm{B}} + \varphi_{l\mathrm{v}} = 1$	α_l
2. normalization	$m(g^{+}_{l\mathrm{K}} + g^{-}_{l\mathrm{K}}) + (1-2m)g^{0}_{l\mathrm{K}} = 1$	$\varphi_{l\mathrm{K}}(\beta_{l\mathrm{K}} - 1)n_{\mathrm{s}}k_{\mathrm{B}}T$
3. flux	$g^{+}_{l\mathrm{K}}\varphi_{l\mathrm{K}} = g^{-}_{l+1,\mathrm{K}}\varphi_{l+1,\mathrm{K}}$	$m\tau_{l\mathrm{K}}n_{\mathrm{s}}k_{\mathrm{B}}T$
4. fixed polymer segments	$n_{\mathrm{K}} = n_{\mathrm{s}}\sum_{l}\varphi_{l\mathrm{K}}$	$\zeta_{\mathrm{K}}n_{\mathrm{s}}k_{\mathrm{B}}T$

The number of voids is not fixed; i.e. it can be varied to minimize the free energy. The flux constraint ensures that the number of bonds going up from layer l equals the number coming down from $l + 1$.

Substituting the full occupancy constraint in the function which has to be minimized and taking the derivatives with respect to $g^{\nu}{}_{l\mathrm{K}}$ give

$$g^{0}{}_{l\mathrm{K}} = \exp(-\beta_{l\mathrm{K}}) \tag{23}$$

$$g^{+}{}_{l\mathrm{K}} = \exp(-\beta_{l\mathrm{K}} - \tau_{l\mathrm{K}}) \tag{24}$$

$$g^{-}{}_{l\mathrm{K}} = \exp(-\beta_{l\mathrm{K}} + \tau_{l-1,\mathrm{K}}) \tag{25}$$

Substituting these equations in the derivative equations and eliminating the Lagrange multiplier α_l leaves the following set of equations to solve (K′ is B if K is A and vice versa)

$$z(1-2m)(\varphi_{l\mathrm{K}}e_{\mathrm{KK}} + \varphi_{l\mathrm{K}'}e_{\mathrm{KK}'}) + zm[(\varphi_{l-1,\mathrm{K}} + \varphi_{l+1,\mathrm{K}})e_{\mathrm{KK}} + (\varphi_{l-1,\mathrm{K}'} + \varphi_{l+1,\mathrm{K}'})e_{\mathrm{KK}'}] - \ln(1 - \varphi_{l\mathrm{K}} - \varphi_{l\mathrm{K}'}) - \beta_{l\mathrm{K}} - 1 - \zeta_{\mathrm{K}} = 0 \tag{26}$$

$$m\exp(-\beta_{l\mathrm{K}} - \tau_{l\mathrm{K}}) + m\exp(-\beta_{l\mathrm{K}} + \tau_{l-1,\mathrm{K}}) + (1-2m)\exp(-\beta_{l\mathrm{K}}) - 1 = 0 \tag{27}$$

$$\varphi_{l\mathrm{K}}\exp(-\beta_{l\mathrm{K}} - \tau_{l\mathrm{K}}) - \varphi_{l+1,\mathrm{K}}\exp(-\beta_{l+1,\mathrm{K}} + \tau_{l\mathrm{K}}) = 0 \tag{28}$$

where $e_{\mathrm{KK}} = -\epsilon_{\mathrm{KK}}/k_{\mathrm{B}}T$. The boundaries of the system are formed by the bulk phases of both polymers, where the densities are found by solving the Sanchez−La-

combe equation of state (once pressure, temperature, and the segment interaction parameters are chosen) and the anisotropy factors are unity, hence $\beta_K^{\text{bulk K}} = 0$. An expression for ζ_K can be found in the bulk since this multiplier is independent of the layer number.

$$\zeta_K = z\varphi_K^{\text{bulk}} e_{KK} - \ln(1 - \varphi_K^{\text{bulk}}) - 1 \qquad (29)$$

The values for β_K in the K′ bulk can be obtained in the same way

$$\beta_K^{\text{bulk K}'} = z\varphi_K^{\text{bulk}} e_{AB} - \ln(1 - \varphi_K^{\text{bulk}}) - 1 - \zeta_{K'} \qquad (30)$$

III. MC Simulation Method

For the simulations an extension of the method used for compressible systems at zero[19,20] and at elevated pressure[21] is used. The method consists of condensing polymer chains against a solid wall, via interactions between chain segments and a short-range adsorption interaction of the wall toward chain segments. The resulting polymer slab is compressible, since the density of the condensed polymer is balanced by the interactions between chains and free exchange of voids between the bulk polymer and the free space above.

A rectangular section of a cubic lattice is used with 60 (50) sites in the *Z*-direction and 24 (22) sites in the other two directions for chain lengths $s = 50$ (30). The solid wall is placed at $Z = 1$ and a system of 500 chains is condensed against this wall. The periodic boundary conditions apply in *X* and *Y* directions. A slab with an A/B polymer interface is prepared in two stages: (1) a homopolymer system is equilibrated as before,[20] and (2) the homopolymer slab is divided into two at a certain *Z* coordinate; the chains with the center of mass smaller than a certain *Z* are assigned A-quality, and those larger or equal are assigned B-quality. After this initial interface is set, the new interaction energies ϵ_{AA}, ϵ_{BB}, and ϵ_{AB} are assigned and, via a new equilibration, a representative interface is produced. Elevated pressures are obtained by applying the scanning piston method:[21] the whole polymer slab is placed under a piston which can be moved (scanning site-by-site) in the *Z*-direction to exert pressure. Although not necessary, the results are converted to real units by choosing $T =$ 300 K and the volume of one site $v^* = 0.0001$ m^3/mol, which closely represents the molar volume of a polystyrene segment. In this *NPT* ensemble we use physical volume fluctuations instead of the common scaling of all distances used for atomic systems. Thus our Metropolis sampling criterion is based on the acceptance probability $p_a = \min(\exp(-(\epsilon\Delta n + P\delta V)/k_BT), 1)$, where

$$\epsilon\Delta n = \epsilon_{11}\Delta n_{11} + \epsilon_{22}\Delta n_{22} + \epsilon_{12}\Delta n_{12} \qquad (31)$$

Δn_{ij} is the change in the number of interactions introduced by a trial move of chains and ΔV is the trial volume change.

Similar simulations have been performed very recently by Muller, Binder, and Oed.[22] These authors consider the effect of vacancies on the polymer/polymer interface. However, their approach utilizes and *NVT* ensemble; i.e. the simulations are performed at a fixed number of vacancies. The present simulations operate in the *NPT* ensemble; consequently, the influence of compressibility is fully accounted for.

IV. Interfacial Tension

The interfacial tension of the system, which is a measure of the strength of the interface, can be calculated from thermodynamics once the concentration profiles are known. It is defined as an excess free energy per unit area[23] and can be derived in two ways depending on how the system is looked upon; both lead to the same result.

Defining the system as consisting of three components gives

$$\gamma_{AB}a^2 = E^{\text{inh}} - TS^{\text{inh}} - \sum_{i=1}^{3}\mu_i N_i \qquad (32)$$

where the chemical potential μ_i of species *i* is by definition the derivative of the Helmholtz free energy with respect to the number of molecules. For the polymer components this leads to

$$\frac{\mu_i}{k_BT} = \left(\frac{\partial A/k_BT}{\partial N_i}\right)_{T,P,N_{j\neq i}} = -(1 - \tilde{\rho}) - \frac{z}{2k_BT}\epsilon_{ii}(\tilde{\rho}^2 - 2\tilde{\rho}) \qquad (33)$$

For the voids this yields the Sanchez−Lacombe equation of state (see eqs 14 and 15):

$$\frac{\mu_{\text{voids}}}{k_BT} = \left(\frac{\partial A/k_BT}{\partial N_v}\right)_{T,N_1,N_2} = v^*\left(\frac{\partial A/k_BT}{\partial V}\right)_{T,N_1,N_2} = -\frac{Pv^*}{k_BT} = \tilde{\rho} + \ln(1 - \tilde{\rho}) + \frac{\tilde{\rho}^2}{\tilde{T}} \qquad (34)$$

Defining the system as two components under pressure gives

$$\gamma_{AB}a^2 = E^{\text{inh}} - TS^{\text{inh}} - \sum_{i=1}^{2}\mu_i N_i + PV \qquad (35)$$

where the chemical potential of the components is defined as

$$\frac{\mu_i}{k_BT} = \left(\frac{\partial G/k_BT}{\partial N_i}\right)_{T,P,N_{j\neq i}} = -(1 - \tilde{\rho}) - \frac{z}{2k_BT}\epsilon_{ii}(\tilde{\rho}^2 - 2\tilde{\rho}) + \frac{Pv^*}{k_BT} \qquad (36)$$

For the MC evaluation of the interfacial tension an approximate formula was presented previously[19]

$$\gamma_{AB}a^2 = 2[(z-2)/z]\sum_l\{\varphi_{l\text{A}}[\epsilon_{AA}(\varphi_{l+1,\text{A}} - \varphi_{l-1,\text{A}}) + \epsilon_{AB}(\varphi_{l+1,\text{B}} - \varphi_{l-1,\text{B}})] - \varphi_{l\text{B}}[\epsilon_{BB}(\varphi_{l+1,\text{B}} - \varphi_{l-1,\text{B}}) + \epsilon_{AB}(\varphi_{l+1,\text{A}} - \varphi_{l-1,\text{A}})]\} \qquad (37)$$

The multiplication factor $(z-2)/z$ takes into consideration effectively only nonbonded contacts.

V. Results and Discussion

To calculate the properties of the pure polymers from *PVT* data, the Sanchez−Lacombe equation of state (SL-EOS) is used. It is known that the Sanchez−Lacombe theory overestimates the MC densities of the pure components. This discrepancy can be removed by introducing a more refined theoretical evaluation of the lattice model using, e.g., the Huggins approximation[2b,24] for the entropy and introducing the effects of nonrandomness, as shown before.[21] The discrepancies between SL-EOS and the MC simulations for the temperature dependence on the reduced bulk density are shown in

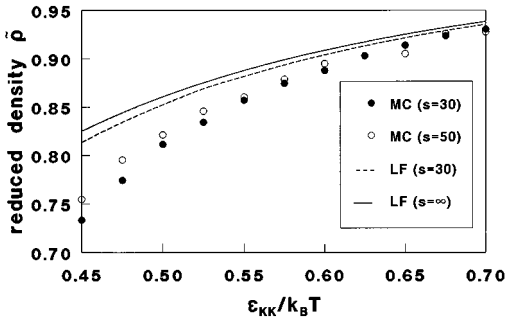

Figure 1. Reduced density $\tilde{\rho}$ (at $P = 0$ bar) of bulk polymers vs the intersegmental interaction parameter ϵ_{KK}/k_BT, a comparison of Monte Carlo simulation and lattice fluid theory.

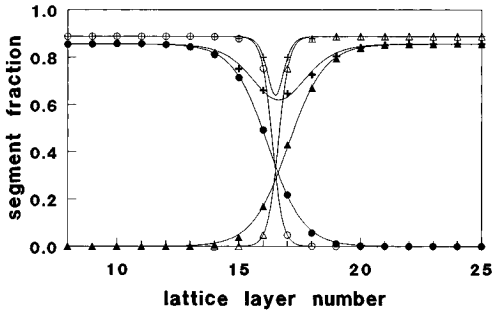

Figure 2. Interfacial profiles for $\epsilon_{AA}/k_BT = \epsilon_{BB}/k_BT = 0.55$, $\epsilon_{AB}/k_BT = 0.35$, a comparison of MC simulation ($s = 30$; (+) total density; (●) polymer A; (▲) polymer B) and LF theory ((+) total density; (○) polymer A; (△) polymer B). Lines are according to eq 38.

Figure 1. We have chosen not to adjust the bulk densities (for instance by varying ϵ_{KK}) but to keep the input parameters the same for both theory and simulation. Evaluating the results, one should keep in mind this discrepancy and the fact that the theory calculations are made for infinite chain length while the simulations are performed with finite chain length. The influence of the chain length will be discussed in relation to the theory of Scheutjens and Fleer.[25]

V.a. Polymer Profiles. An example of polymer profiles is shown in Figure 2. The symbols in this figure represent the calculated and simulated segment fractions of the polymers on the lattice layers and the reduced density. The lines in these figures are fitted with the usual interface profile function[26]

$$\varphi_{lK} = \frac{\varphi_{K,bulk}}{2}\left[1 \pm \tanh\left(\frac{2(l - d_K)}{D_K}\right)\right] \qquad (38)$$

where d_K and D_K are the position and the thickness and full width of the interface, respectively.

There is some asymmetry in MC profiles due to the finite amount of polymer used in the simulation, as a result of which the interface is floating with the amount of material used and not necessarily between two layers. The finite amount of material in the MC simulations means that the compressible interface shifts by varying interactions or applying the pressure, and this poses problems for the comparison with the LF calculations. However, this does not mean that the MC system is too small to produce representative results for the bulk and interface properties. This was confirmed in a previous paper.[21]

Both Monte Carlo simulations and the theory show a density dip at the interface between the polymers. While this density fluctuation costs free energy, it reduces unfavorable polymer−polymer contacts. The theoretical polymer concentration profiles are sharper compared to the MC simulation results and also the theoretical density dip is narrower. At this point it should be noted that the results of Muller, Binder, and Oed show the same trend: the simulated profiles are approximately twice as broad if compared to theoretical calculations.[22] Several causes for these discrepancies can be thought of, such as the difference in bulk density, configurational entropy effects, correlations, and excluded volume effects not taken into account in the mean field approach. In general, a lower bulk density leads to a broader interface. This effect contributes to the broadening of the interface found for the simulations, but this contribution is not sufficient to explain the observed difference. The simulations are done for 30 and 50 mers, whereas the calculations are for infinite chain length. Chains of finite length have also so-called configurational entropy, associated with the translational degrees of freedom, in addition to the conformational entropy considered in the present theory, which may cause the chains to move away from the interface. The influence of chain length, although not included in the present theory, can be studied by, e.g., the self-consistent field theory of Scheutjens and Fleer. This approach, similar to the one considered here, includes the chain length effects in the configurational entropy using the Flory approximation. More details about this theory and a comparison with several other theoretical approaches can be found in ref 25. Calculations based on this theory were kindly performed by F. A. M. Leermakers and show only a very small influence of chain length on the concentration profiles, the density dip, and the overall width of the interface. Therefore the observed difference in the interfacial width between simulation and theory cannot be ascribed to the difference in chain length used. This would mean that the broadening of the interface for the simulations is mainly due to correlation and excluded volume effects not accounted for in the mean field theories considered here.

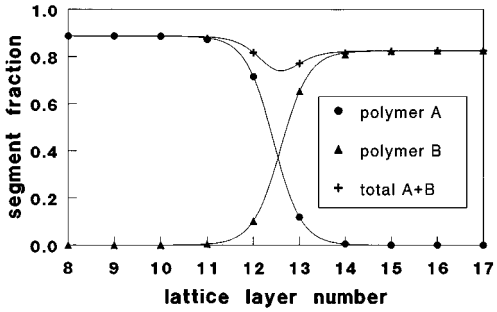

Figure 3. Interfacial profiles from LF theory of an asymmetric polymer blend, $\epsilon_{AA}/k_BT = 0.55$, $\epsilon_{BB}/k_BT = 0.45$, and $\epsilon_{AB}/k_BT = 0.40$: (+) total density; (●) polymer A; (▲) polymer B. Lines are according to eq 38.

The theoretical calculations and the MC simulations can be performed for density asymmetric systems. An example of the resulting theoretical interfacial polymer profiles is given in Figure 3.

The pressure dependence of the polymer profiles is shown in Figure 4. For the MC results in Figure 4a it is seen that the density of the homopolymers increases with increasing pressure and the location of the interface shifts as a result of the scanning piston method due to the finite amount of material, as mentioned before. The dip decreases with increasing pressure and increasing A−B contact energy, as expected. The same behavior is found for the theory shown in Figure 4b. For the

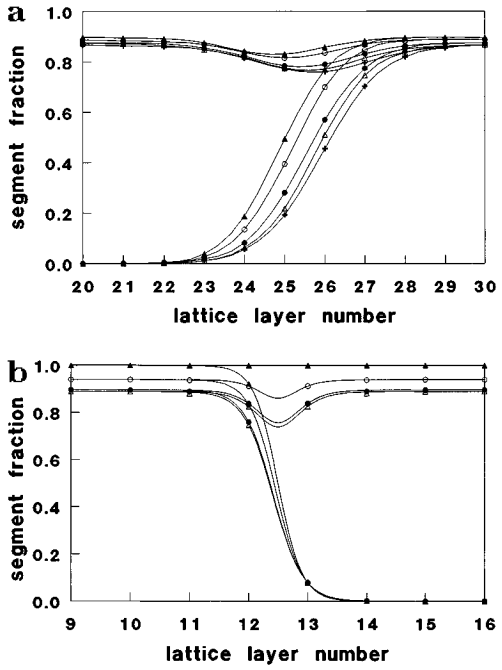

Figure 4. (a) Pressure dependence of the interfacial profiles from MC simulations ($s = 50$) for $\epsilon_{AA}/k_BT = \epsilon_{BB}/k_BT = 0.55$ and $\epsilon_{AB}/k_BT = 0.41$. The segment fraction of one of the polymers and the reduced density are shown for $P = 2$ (+), 5 (△), 10 (●), 20 (○), and 40 (▲) bar. Lines are drawn for convenience. (b) Pressure dependence of the interfacial profiles from LF theory for $\epsilon_{AA}/k_BT = \epsilon_{BB}/k_BT = 0.55$ and $\epsilon_{AB}/k_BT = 0.41$. The segment fraction of one of the polymers and the reduced density are shown for $P = 1$ (△), 10 (●), 100 (○), and 1000 bar (▲). Lines according to eq 38.

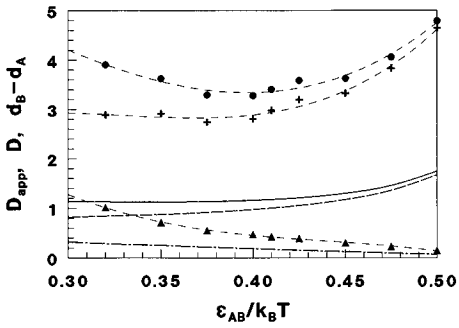

Figure 5. Apparent interface thickness D_{app} (●), D (+), and $d_B - d_A$ (▲) according to eq 38 vs the intersegmental interaction parameter ϵ_{AB}/k_BT. MC simulation ($s = 30$): symbols and dashed lines. Theory ($\epsilon_{AA}/k_BT = \epsilon_{BB}/k_BT = 0.55$): D_{app} (—), D (– – –), and $d_B - d_A$ (–·–).

theoretical calculations we can go to extremely high pressures where the reduced density of the bulk polymers approaches unity and the density dip vanishes, recovering Helfand's results for incompressible systems.

In Figure 5 different definitions of interfacial thickness are shown for the symmetrical polymer/polymer interface as a function of the cross interaction ϵ_{AB}. The total thickness of the interface D_{app} is defined as the sum of two contributions, i.e. the thickness of the concentration profile defined by D_K and the difference of the positions $d_B - d_A$ of the A-polymer and B-polymer profile, both obtained from eq 38. If the cross interaction ϵ_{AB} approaches the pure component interaction ϵ_{KK}, the concentration profiles become broad due to the improved miscibility whereas the separate concentration profiles approach each other, leading to an increase in the total interfacial thickness. On the other hand for small cross interactions the concentration profiles become narrow but the separate profiles tend to repel, also leading to an increase in total interfacial thickness. This increased interfacial thickness at small cross interactions does not indicate the existence of a "good" interface but is the result of the extreme effective repulsion of the two components. For intermediate cross interaction a minimum in the total interfacial thickness is observed. Although the absolute width of the interface is consistently smaller for the theory calculations, it is shown that both simulation and theory show a very similar behavior.

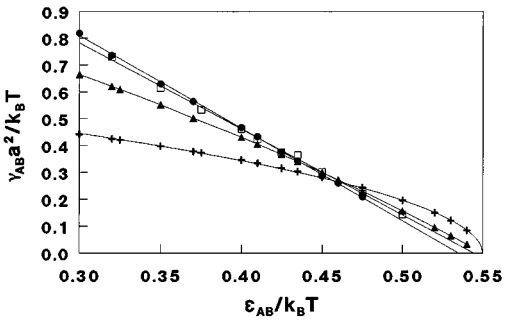

Figure 6. Interfacial tension γ_{AB} vs the intersegmental interaction parameter ϵ_{AB}/k_BT, a comparison of MC simulation ($s = 50$) using eq 45 for $s = 30$ (●) and $s = 50$ (□) and LF theory using eq 45 (▲) and eq 40 (+).

V.b. Interfacial Tension. The interfacial tensions are calculated, and the results are plotted in Figure 6 as a function of the A−B contact energy ϵ_{AB}. The plot shows an almost linear dependence for the simulation using the approximate eq 37. Using a consistent theoretical calculation for the interfacial tension by eq 32, a square root like behavior is found for the interfacial tension as function of the A−B contact energy, in agreement with Helfand.[3] These results cannot be compared directly to the simulation results for the interfacial tension. Theory and simulation can be compared if eq 37 is also used to evaluate the theoretical results. In this case the agreement between theory and simulation improves considerably and an almost linear behavior of the interfacial tension versus ϵ_{AB} is observed also theoretically. However, it should be noted that eq 37 is only approximate, thus leading to quantitatively erroneous results. At present the correct evaluation of the surface tension from the simulations remains to be done and the linear dependence must be interpreted with some care.

V.c. Chain Ends. Figures 7−9 depict microscopic details of the interface related to the behavior of individual coils across the interface. The selected situation represents the interface with a realistic density dip for $\epsilon_{AA} = \epsilon_{BB} = 0.55k_BT$, $\epsilon_{AB} = 0.41k_BT$, and $s = 50$. In Figure 7 the segregation of chain ends into the interfacial region is shown relative to the average segment density. Both chain ends and average segment density profiles are scaled to unity in the bulk region. This enrichment of the interface by chain ends can be visualized by plotting the difference of two respective profiles. This behavior was predicted by theory.[27] It is related to a different chain length dependence of surface tension from bulk properties and is in agreement with recent simulation results.[28−30] Olaj et al.[31] showed this effect for an incompressible polymer/polymer interface. Here we present results on a compressible system with a reasonable dip at the interface.

V.d. Coil Centers of Mass. The situation of the chain centers of mass is shown in Figure 8. It is clearly seen that there is a layering effect at the interface. In

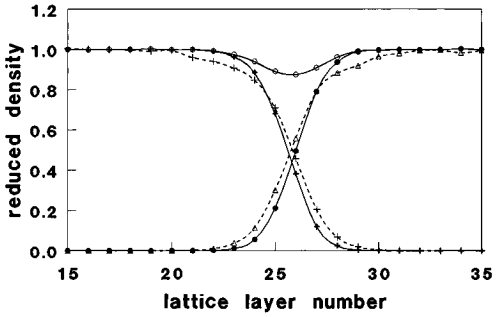

Figure 7. Interfacial profiles showing the average segment density and the total density (—) and chain end segment density (- - -), all scaled to unity in the bulk region. (MC: $s = 50$, $\epsilon_{AA}/k_BT = \epsilon_{BB}/k_BT = 0.55$, $\epsilon_{AB}/k_BT = 0.41$.)

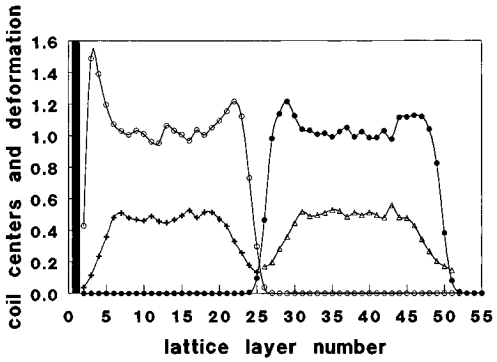

Figure 8. Interfacial profiles showing the relative coil center density (A (○), B (●)) and the coil deformation and orientation factor in terms of $\langle R^2\rangle_Z/(\langle R^2\rangle_X + \langle R^2\rangle_Y)$ for both polymers (A (+), B (△)). The thick line at $l = 1$ represents the solid wall to which the two-layered polymer slab is condensed. (MC: $s = 50$, $\epsilon_{AA}/k_BT = \epsilon_{BB}/k_BT = 0.55$, $\epsilon_{AB}/k_BT = 0.41$.)

the middle of the interface or close to the hard wall only a limited number of coil centers is found, while there is an enhancement of centers next to the interface. It can be noticed that the distance of the layer of centers from the middle of the interface is approximately one radius of gyration R_G of the coils. The average end-to-end distance in the bulk polymer from MC is $\langle R^2\rangle = 77.5$. Using a Gaussian chain approximation we obtain $R_G = 3.59$. A very similar value $R_G = (b^2N/6)^{1/2} = 3.54$ is obtained by assuming our chains as random walks on a five-choice cubic lattice, which corresponds to an average valence angle $\langle\cos(\varphi)\rangle = -0.2$ and a Kuhn segment length $b = 1.5^{1/2}$.

If we compare the layering at the solid wall and at the interface, it is obvious that at the wall the effect is stronger and the layer of centers is closer to the solid wall. This is related to deformation and orientation of coils at both interfaces which is stronger at the wall. Figure 8 depicts also the deformation of coils in terms of the ratio $\langle R^2\rangle_Z/(\langle R^2\rangle_X + \langle R^2\rangle_Y)$. In the bulk region where a random orientation prevails and no deformation of coils is found, the ratio is 0.5 while at both types of interfaces both orientation and deformation is seen by the decrease of its values below 0.5, which indicates a pancake shape of coils which are flattened and parallel to the interfaces. This is also noticed by Szleifer and Widom.[32]

V.e. Segmental Contacts. Interesting features are revealed by looking at different types of contacts at the interface profile. Figure 9 plots profiles with three types of contacts for each component: segment—segment homocontact, heterocontact, and segment—void "contact". The sum of all types is 6 for each layer l and each

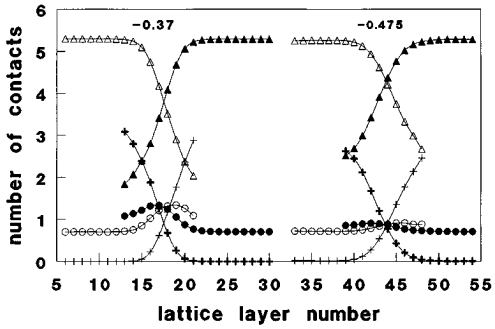

Figure 9. Homosegment contacts (△), heterosegment contacts (+), and void-segment contacts (○) across the interface for two different cross interaction parameters $\epsilon_{AB}/k_BT = 0.37$ and $\epsilon_{AB}/k_BT = 0.475$, where the latter profiles are shifted by $\Delta l = 27$. (MC: $s = 30$, $\epsilon_{AA}/k_BT = \epsilon_{BB}/k_BT = 0.55$.)

component. The first two types of contacts closely resemble the density profile. The segment—void "contact" shows that a segment is surrounded by more voids in the interface region (in accordance with the existence of a density dip) but also that it is surrounded by more voids at a side of the other phase of the interface. This can be explained by the fact that there is a repulsion between different types of segments, and thus the other type of segment is likely to give up the neighbor position in favor of voids. It should be noted that at the interface the statistics of sampling are inevitably poorer for the component which has a small concentration. Consequently, certain properties—such as segmental contacts—are difficult to obtain accurately. Hence, the curves in Figure 9 were terminated in the interfacial region whenever the concentration of the minority component was less than 3% of the bulk density.

VI. Conclusions

A mean field lattice theory is presented for compressible polymer—polymer systems which is not restricted to broad interfaces. The theory allows for the treatment of polymer pairs with symmetric as well as asymmetric interactions. So far the theory has been developed for infinite chain lengths which results in a considerable simplification since no configurational entropy effects are present. Although the theory is also valid for sharp interfaces, its application to real systems in this case should be done with care, as the applicability of the lattice model itself to these situations is questionable.

The main feature of the theory is the occurrence of a density dip at the polymer—polymer interface when the polymers exhibit a finite compressibility. In addition, when pressure is applied, the density dip decreases and at full occupancy the incompressible results of Helfand are recovered. The influence of compressibility was addressed already in an *ad hoc* manner in the original papers of Helfand.[26a] In the present contribution the compressibility is treated in a theoretically consistent manner.

Theory and simulation for the same model of molecular interactions (i.e. the lattice model with nearest neighbor interactional constants) are in qualitative or even semiquantitative agreement. The observed differences between theory and simulation for the chain lengths and interactional constants considered in this study are not due to the finite chain lengths involved in the simulation. This was proven by comparing the results for the infinite chain length theory to those of the self-consistent field theory of Scheutjens and Fleer which does include configurational entropy effects. The

results of the infinite chain length calculations and the self-consistent field theory of Scheutjens and Fleer are virtually identical. It is expected that the observed differences are related to correlations present in the simulations but neglected in the mean field theory.

The interfacial thickness as a function of cross interactional constant is evaluated by simulation and theory. At relatively small effective repulsions the expected square root dependence on the Flory−Huggins interaction parameter is observed in both cases. However, upon an increase in the effective repulsion (increasing immiscibility) the interfacial thickness has a minimum and increases again. In the simulation this increase is much more pronounced than in the theory.

The interfacial tension is evaluated theoretically and by simulation. The theoretical evaluation of the interfacial tension is done according to two equations. The correct theoretical expression for the interfacial tension gives the expected square root dependence with the cross interactional constant, whereas the use of an approximate equation, presented previously, and used also for the simulation results on previous occasions, has a qualitatively different behavior. From this it must be concluded that the approximate equation is incorrect and the results obtained with this equation should be considered with care. A correct evaluation of the interfacial tension of the MC simulation results remains to be done.

Finally, detailed microscopic properties such as coil center of mass location, coil orientation, and segmental contacts at the interface are presented. Near the interface coil centers of mass are preferentially found at a distance of the radius of gyration. Furthermore the coils are oriented with their longest axis perpendicular to the interface. The occurrence of the different types of segmental contacts are in agreement with the presence of the density dip.

Acknowledgment. We thank Dr. Frans A. M. Leermakers from the Department of Physical and Colloid Chemistry of the Wageningen Agricultural University for the evaluation of the chain length effect with the Scheutjens & Fleer self-consistent field theory. Early simulations of the interface profile with the density dip were obtained while P.C. was staying with F. E. Karasz at the University of Massachusetts.

References and Notes

(1) Flory, P. J. *Principles of Polymer Chemistry*; Cornell University Press: Ithaca, NY, 1953.
(2) (a) Flory, P. J. *J. Chem. Phys.* **1941**, *9*, 440. (b) Huggins, M. L. *J. Chem. Phys.* **1941**, *9*, 660.
(3) Helfand, E. *J. Chem. Phys.* **1975**, *63*, 2192.
(4) Helfand, E. *Macromolecules* **1976**, *9*, 307.
(5) Weber, T. A.; Helfand, E. *Macromolecules* **1976**, *9*, 311.
(6) Poser, C. I.; Sanchez, I. C. *J. Colloid Interface Sci.* **1979**, *69*, 539.
(7) Cahn, J. W.; Hilliard, J. E. *J. Chem. Phys.* **1958**, *28*, 258.
(8) Cahn, J. W. *J. Chem. Phys.* **1959**, *30*, 1121.
(9) Hong, K. M.; Noolandi, J. *Macromolecules* **1981**, *14*, 1229.
(10) Helfand, E. *J. Chem. Phys.* **1975**, *62*, 999.
(11) (a) Sanchez, I. C.; Lacombe, L. H. *Macromolecules* **1978**, *11*, 1145. (b) Sanchez, I. C.; Panayiotou, C. G. *Models for Thermodynamic and Phase Equilibria Calculations*; Sandler, S. I., Ed.; Marcel Dekker Inc.: New York, 1994.
(12) Lifschitz, M.; Freed, K. F. *J. Chem. Phys.* **1993**, *98*, 8994.
(13) Leibler, L. *Macromolecules* **1980**, *13*, 1602.
(14) Theodorou, D. N. *Macromolecules* **1989**, *22*, 4578, 4589.
(15) Hariharan, A.; Kumar, S. K.; Russell, T. P. *J. Chem. Phys.* **1993**, *98*, 6516; *99*, 4041.
(16) Rowlinson, J. S.; Widom, B. *Molecular Theory of Capillarity*; Clarendon Press: Oxford, U.K., 1972.
(17) Chandler, P.; McCoy, J. D.; Singer, S. J. *J. Chem. Phys.* **1986**, *85*, 5971.
(18) Yethiraj, A.; Woodward, C. E. *J. Chem. Phys.* **1995**, *102*, 5499.
(19) Cifra, P.; Karasz, F. E.; MacKnight, W. J. *Macromolecules* **1992**, *25*, 4895.
(20) Cifra, P.; Nies, E.; Karasz, F. E. *Macromolecules* **1994**, *27*, 1166.
(21) Nies, E.; Cifra, P. *Macromolecules* **1994**, *27*, 6033.
(22) Muller, M.; Binder, K.; Oed, W. *J. Chem. Soc., Faraday Trans.* **1995**, *91*, 2369.
(23) (a) *The collected works of J. Willard Gibbs*; Longmans, Green: London, 1928−1931; Vol. 1. (b) Sanchez, I. C. *Physics of Polymer Surfaces and Interfaces*; Manning Publications Co.: Boston, 1992.
(24) Hertanto, A.; Dickman, R. *J. Chem. Phys.* **1988**, *89*, 7577.
(25) Fleer, G. J.; Stuart, M. A.; Scheutjens, J. M. H. M.; Cosgrove, T.; Vincent, B. *Polymers at Interfaces*; Chapman & Hall: London, 1993.
(26) (a) Helfand, E.; Tagami, Y. *J. Chem. Phys.* **1972**, *56*, 3592. (b) Helfand, E.; Tagami, Y. *Ibid.* **1972**, *57*, 1812.
(27) de Gennes, P. G. *J. Phys.* **1989**, *50*, 2551.
(28) Theodorou, D. N. *Macromolecules* **1988**, *21*, 1391.
(29) Kumar, S. K.; Vacatello, M.; Yoon, D. Y. *Macromolecules* **1990**, *23*, 2189.
(30) Bitsanis, I.; Hadziioannou, G. *J. Chem. Phys.* **1990**, *92*, 3827.
(31) Reiter, J.; Zifferer, G.; Olaj, O. F. *Macromolecules* **1990**, *23*, 224.
(32) Szleifer, I.; Widom, B. *J. Chem. Phys.* **1989**, *90*, 7524.

MA9509568